



Geophysical Research Letters®

RESEARCH LETTER

10.1029/2024GL108292

Key Points:

- The observed Equatorial Pacific cooling trend, unpredicted by climate models, may have led to decreased precipitation in the southwestern US
- With a sea surface temperature–precipitation Green's function, we find that small changes in sea surface temperature can either wet or dry the southwestern US
- A reversal of the cooling trend in the Equatorial Pacific could lead to a wetting trend in the southwestern US

Supporting Information:

Supporting Information may be found in the online version of this article.

Correspondence to:

M. J. Alessi,
marc.alessi@colostate.edu

Citation:

Alessi, M. J., & Rugenstein, M. (2024). Potential near-term wetting of the Southwestern United States if the Eastern and Central Pacific cooling trend reverses. *Geophysical Research Letters*, 51, e2024GL108292. <https://doi.org/10.1029/2024GL108292>

Received 11 JAN 2024

Accepted 20 JUN 2024

Potential Near-Term Wetting of the Southwestern United States if the Eastern and Central Pacific Cooling Trend Reverses

Marc J. Alessi¹  and Maria Rugenstein¹ 

¹Department of Atmospheric Science, Colorado State University, Fort Collins, CO, USA

Abstract Near-term projections of drought in the southwestern United States (SWUS) are uncertain. The observed decrease in SWUS precipitation since the 1980s and heightened drought conditions since the 2000s have been linked to a cooling sea surface temperature (SST) trend in the Equatorial Pacific. Notably, climate models fail to reproduce these observed SST trends, and they may continue doing so in the future. Here, we assess the sensitivity of SWUS precipitation projections to future SST trends using a Green's function approach. Our findings reveal that a slight redistribution of SST leads to a wetting or drying of the SWUS. A reversal of the observed cooling trend in the Central and East Pacific over the next few decades would lead to a period of wetting in the SWUS. It is critical to consider the impact of possible SST pattern trends on SWUS precipitation trends until we fully trust SST evolution in climate models.

Plain Language Summary Precipitation trends in the southwestern United States (SWUS) are sensitive to the pattern of sea surface temperature (SST) trends in the Tropical Pacific. Since the turn of the century, a decrease in SWUS precipitation has been linked to a cooling of the Central and Eastern Pacific (1990–2020). Notably, climate models are unable to simulate this observed cooling SST trend. In this study, we answer how SWUS precipitation projections may be impacted by potential error in the simulation of future SST trends by climate models. We first demonstrate that slight changes in the pattern of SST trends leads to either a wetting or drying of the SWUS. Second, if the current 30-year cooling trend in the Central and East Pacific switches to a warming trend, the SWUS could experience a near-term increase in precipitation. While climate models are the main tool to predict the global response to anthropogenic climate change, we must consider and account for their error in projections of global warming.

1. Introduction

As anthropogenic climate change continues, the risk of drought is expected to increase in the southwestern United States (SWUS), home to nearly 60 million people, mainly due to an increase in evapotranspiration and an overall drying of soils due to higher temperatures (Ault, 2020; Cook et al., 2014). In fact, a severe, multi-decadal drought, known as a “megadrought,” is ongoing since the beginning of the 21st century in the SWUS (Cook et al., 2021; Williams et al., 2022). Rather than being caused by increased evapotranspiration from warming, this drought developed from a decrease in precipitation due to a combination of internal atmospheric variability and forcing from sea surface temperature (SST) anomalies in the Equatorial Pacific (Lehner et al., 2018; Seager et al., 2015). Here, we focus on how long-term SST trends (30-year trends) drive SWUS precipitation trends in projections.

It is well established that the SWUS hydroclimate is sensitive to Tropical Pacific SST patterns, with the El Niño–Southern Oscillation (ENSO) being a dominant driver of interannual hydroclimate variability for the SWUS (e.g., Evans et al., 2022; Hoerling et al., 1997; Piechota & Dracup, 1996; Redmond & Koch, 1991). Warmer SSTs in the Central and East Pacific, which are characteristic of a warm-phase ENSO event (referred to as an El Niño), shift the area of deep convection eastward from the West Pacific warm pool to the Central Pacific. The area of peak divergence then shifts in the upper tropical troposphere, thus exciting midlatitude Rossby waves (Horel & Wallace, 1981; Sardeshmukh & Hoskins, 1988). This results in an extension of the northern subtropical Pacific jet, bringing anomalous moisture and precipitation to the SWUS (Deser et al., 2018; Hu et al., 2021; Ropelewski & Halpert, 1986; Seager et al., 2010). While the ENSO phase is a helpful predictor of the SWUS hydroclimate, the precipitation response is nonlinear with respect to temperature (Hoerling & Kumar, 2002; Hoerling et al., 1997; Seager et al., 2015), meaning that a change in SWUS precipitation does not scale linearly with a change in SST. A warming in the East Pacific (El Niño) results in an increase in precipitation in the SWUS, while the impacts of a

© 2024. The Author(s).

This is an open access article under the terms of the [Creative Commons Attribution License](#), which permits use, distribution and reproduction in any medium, provided the original work is properly cited.

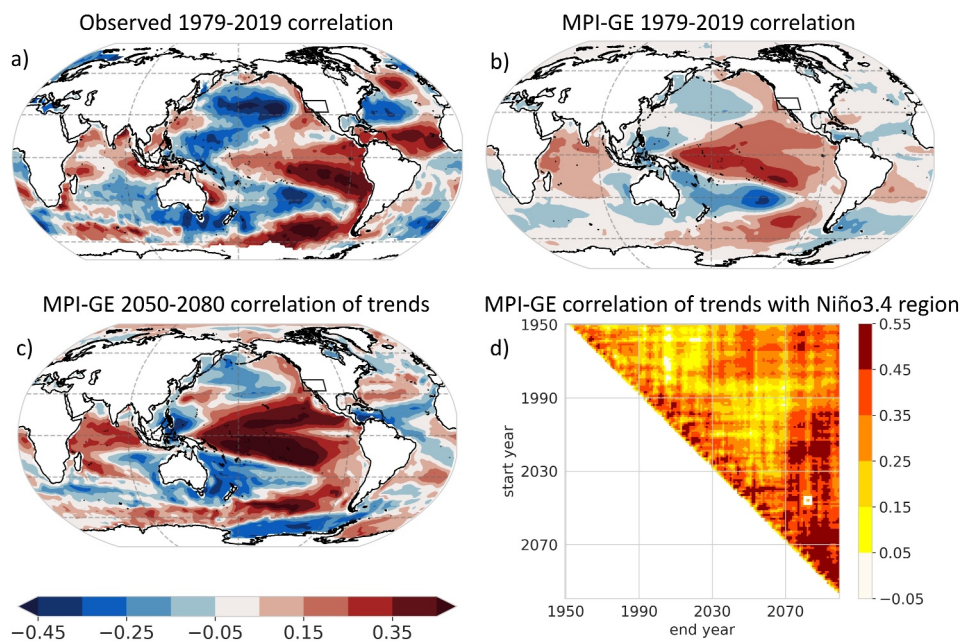


Figure 1. (a) The observed 1979–2019 correlation between annual-mean Southwestern United States (SWUS) precipitation (Global Precipitation Climatology Project) and sea surface temperature (SST; HadISST) at each grid point. (b) The simulated 1979–2019 correlation between annual-mean SWUS precipitation (32° – 40° N, 124° – 105° W) and SST at each grid point in the MPI-GE. Correlation is first calculated across 1979–2019 within each ensemble member and then the average of the ensemble is taken. (c) Correlation between the trends in SWUS precipitation and SST at each grid point for years 2050–2080 in the MPI-GE Representative Concentration Pathway 8.5 (RCP8.5) scenario. The trend is first calculated within each ensemble member, and then the correlation is taken across the ensemble. The color bar in (c) applies to (a) and (b) as well. (d) Correlation between the trends in SWUS precipitation and Niño3.4 region (5° S– 5° N, 170° – 120° W) SST for different start and end years when calculating the trend. The small white box in (d) denotes the situation in panel (c).

cooling East Pacific (La Niña) are less certain (Seager et al., 2015) but tend to lead to SWUS drying (Carrillo et al., 2022). Furthermore, internal atmospheric variability has a larger role than SST forcing in explaining SWUS precipitation variance, as most historical droughts are unrelated to SST forcing (Cook et al., 2018; Schubert et al., 2016; Seager et al., 2015). In observations, SWUS precipitation is moderately positively correlated to changes in Equatorial Pacific SST (Figure 1a). This correlation also exists in the Max Planck Institute Earth System Model Grand Ensemble (MPI-GE), though to a lesser extent in the average of the 100 ensemble members (Figure 1b).

Dettinger et al. (1998) found that the relationship between Tropical Pacific SST and SWUS precipitation on interannual timescales (2–7 years) holds for decadal timescales (7+ years) in observations, that is, a decadal-long cooling trend in the East Pacific is linked to long-term drying in the SWUS. Schubert et al. (2016) and Seager and Hoerling (2014) confirmed a link between long-term trends (decades long) in SST and SWUS precipitation during the historical era using prescribed SST atmospheric general circulation model (A-GCM) simulations across different models. We find a similar relationship in the MPI-GE (Figure 1d): a moderate correlation exists between SWUS precipitation trends and Central Pacific SST trends for the historical period (starting and ending years pre-2014). Furthermore, some decades are correlated while others are not at all (e.g., 1960–1990 has a higher correlation than 1970–2000), meaning that studies focusing on one timescale might over- or underpredict the link between SWUS precipitation and Central Pacific SSTs. Longer trends are generally more strongly correlated (top right of Figure 1d), and trends should be taken over longer periods than 20 years to avoid noise (diagonal of Figure 1d). This dependence of SWUS precipitation trends on Tropical Pacific SST trends suggests possible skill in predicting SWUS precipitation based on the long-term SST trend in the Tropical Pacific. Naturally, this skill in projecting SWUS precipitation exists only if atmosphere-ocean general circulation models (AO-GCMs) correctly simulate the SST trend pattern.

Unfortunately, AO-GCMs fail to replicate the observed SST trend pattern in the Tropical Pacific for many time periods since 1950 (e.g., Rugenstein et al., 2023; Wills et al., 2022). The observed cooling trend (1990–2020) in

the East and Central Pacific not replicated by historical simulations in AO-GCMs could indicate that models' response to anthropogenic forcing is erroneous (e.g., Heede & Fedorov, 2021; Seager et al., 2019) or that their range of internal variability is too small (Olonscheck et al., 2020; Watanabe et al., 2021). The Eastern Pacific is in fact warming in trends starting after 1995—although we do not know whether this is due to internal variability or the forced response to greenhouse gases or aerosols. The current warming could be a signal of an advanced forced response to greenhouse gases (Heede et al., 2020). By initializing AO-GCMs with observed wind-stress anomalies in the Tropical Pacific, Delworth et al. (2015) found that models could replicate the observed cooling trend in the Central and East Pacific, which then resulted in a tropical dynamical setup conducive for development of SWUS drought. Given the relationship between Tropical Pacific SST and SWUS precipitation trends, we here analyze how a likely near-term warming trend in the Central and East Pacific might affect SWUS precipitation.

In this paper, we: (a) test the sensitivity of SWUS precipitation trends by slightly adjusting the likely erroneous near-future SST trends an AO-GCM produces by its free ocean-atmosphere interaction and (b) predict a wetting trend in the SWUS over the next few decades if the cooling trend in the East Pacific reverses. We do not attempt to argue whether the erroneously simulated SST trends in the Tropical Pacific are due to model errors in the forced response or due to an incorrect representation of internal variability. Given that modeled trends in SST are incorrect over the last few decades, we ask how SST trends affect SWUS precipitation in the future if this model error continues or abates.

2. Methods

We developed a precipitation Green's function (GF_P) to identify which SST regions influence SWUS (32° – 40° N, 124° – 105° W) precipitation (e.g., Alessi & Rugenstein, 2023b; Bloch-Johnson et al., 2024; Y. Dong et al., 2019; Zhang et al., 2023; Zhou et al., 2017). We selected this region based on previous work (Evans et al., 2022), and our results do not depend on changes to the box within a reasonable definition of the SWUS. A GF is derived from multiple simulations of one A-GCM where anomalous SST patch perturbations are prescribed locally while elsewhere the SST is kept constant (see Text S1 and Figure S1 in Supporting Information S1 for details on the development of the GF). The GF is developed using the response averages over 20 years to a constant local SST forcing, making the tool ideal for studying the relationship of long-term trends in SST and precipitation. A GF is advantageous to using a coupled AO-GCM or uncoupled A-GCM because atmospheric variability is removed when calculating the precipitation response, that is, we can causally attribute a precipitation response directly to a change in local SST. When using an AO-GCM or A-GCM, atmospheric noise makes the connection less obvious and causal attribution of precipitation more difficult. For example, in A-GCM simulations with a complete spatial and temporal SST pattern prescribed, as in Schubert et al. (2016) and Seager and Hoerling (2014), the precipitation response is a result of both a change in the SST pattern and fluctuations in atmospheric variability and hence sensitively depends on the timing of trend analyses, even for trends over several decades (Figure 1d). In addition, precipitation changes cannot be attributed to one specific region as the whole pattern is prescribed.

The global-mean GF_P is quantitatively similar to GF_P in Zhang et al. (2023; not shown). In this study, we utilize a regional GF_P to focus only on SWUS precipitation response to SST (Figure 2a). Precipitation in the SWUS is most sensitive to changes in SST in the Central Pacific and the Caribbean (Figure 2a), which corroborates the moderate correlation between SWUS precipitation and Central Pacific SST (Figure 1c). An increase in SST in the Central Pacific (denoted by green in Figure 2a) leads to more precipitation in the SWUS. The opposite is true for the Caribbean (denoted by brown in Figure 2a). This result qualitatively confirms the GF work by Barsugli and Sardeshmukh (2002), confirms the well-studied teleconnection to the Central Pacific (e.g., Hoerling et al., 1997; Redmond & Koch, 1991), and backs empirical orthogonal analysis of SST and SWUS precipitation (Hu et al., 2021). Note that while we do not trust the SST pattern in AO-GCMs, we, in principle, trust the link between SST and precipitation trends because models reproduce observational precipitation given the SST pattern (Dettinger et al., 1998; McCabe et al., 2004).

We “tune” GF_P to reproduce the SWUS precipitation output from the historical and RCP8.5 MPI-GE ensemble-mean simulations (Figure 2b), similar to Y. Dong et al. (2019) and Alessi and Rugenstein (2023b). Without tuning, the GF predicts too much wetting in the SWUS (Figure S2 in Supporting Information S1). While GF_P identifies physically meaningful SST regions as impactful to SWUS precipitation, it probably overestimates the SWUS precipitation response given a warming in the Central Pacific due to nonlinearities of the climate system

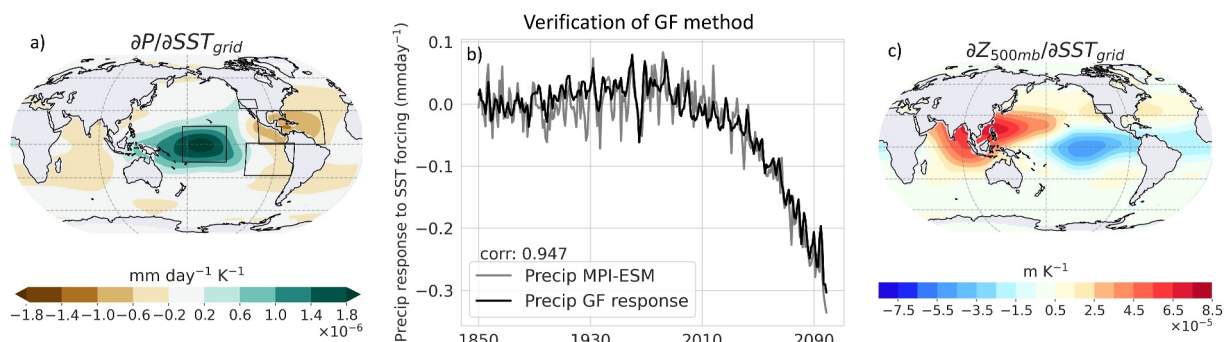


Figure 2. (a) The annual-mean SWUS precipitation response per unit sea surface temperature (SST) warming in each grid box. A warming in a green (brown) region on this map results in an increase (decrease) in precipitation over the SWUS. From the northernmost box going clockwise: the SWUS (32° – 40° N, 124° – 105° W), Caribbean region (0° – 30° N, 107° – 40° W), East Pacific region (28° S– 1° N, 120° – 71° W), and Central Pacific region (16° S– 16° N, 175° E– 140° W). (b) The SWUS precipitation response of the Green's function convolved with the MPI-GE SST pattern (black) reproducing the SWUS precipitation output from the MPI-GE historical and RCP8.5 simulations (gray). (c) The annual-mean 500 mb geopotential height response averaged over the SWUS region per unit SST warming in each grid box.

that GF_P cannot capture (Williams et al., 2023). We correct this error in GF_P by subtracting the same small value (8.6×10^{-5}) from each index of the GF_P matrix. Our results hold qualitatively for the untuned GF_P and for different choices of tuning, since the tuned GF_P has the same pattern as the original GF_P , so a warming in the Central Pacific (Caribbean) still results in a wetting (drying) of the SWUS. We discuss different tuning methods in Text S2 of Supporting Information S1 in depth. So far, GFs have been used only to calculate a climate response in the global-mean. In this study, we use a regional GF that is tuned for a specific range of SST and precipitation variations, that is, for surface temperature variations of a few K and precipitation responses of a few tenths of mm day^{-1} . Tuning and applying a regional GF is a much more stringent use of the tool than the global-mean GF for radiation, which works well for situations very different from the one it was constructed for.

We develop a 500 mb geopotential height Green's function (GF_Z), a 200 mb u -wind Green's function (GF_u), and a 200 mb v -wind Green's function (GF_v) to verify if GF_P changes precipitation in the SWUS as a result of warming in the Central Pacific for the right dynamical reasons. How the subtropical jet stream responds to changes in the SST pattern is explained by GF_Z (Figure 2c), GF_v , and GF_u (Figure S3 in Supporting Information S1), which represent the location of troughs and ridges, meridional displacement of the jet stream, and intensity of the jet stream, respectively. A warming of the Central Pacific decreases both the v -wind at 200 mb and the geopotential height over the SWUS, indicating a southward shift of the subtropical jet stream from the Pacific Northwest and a deepening trough over the SWUS, respectively, which allow for an increase in precipitation in the SWUS. These dynamical GF sensitivity maps confirm a path for increased precipitation in the SWUS given a warming in the Central Pacific (e.g., Hu et al., 2021; Seager et al., 2010).

In the following, we adjust SST trend patterns by cooling and warming the SST trend in the Caribbean, the Central Pacific, and the East Pacific to test the sensitivity of SWUS precipitation to SST in these regions (Section 3.1). We then develop plausible future SST pattern storylines starting from observations and calculate the SWUS precipitation response to these SST patterns using GF_P (Section 3.2).

3. Results

3.1. Sensitivity of SWUS Precipitation Trends to SST Trends

We adjust the SST trend in different regions to quantitatively assess the impact corrected (or more likely correct) SST trends have on SWUS precipitation. We first test six idealized scenarios: a cooler and warmer Caribbean, a cooler and warmer Central Pacific, and a cooler and warmer East Pacific than the RCP 8.5 MPI-GE simulations. In each region, an equally large area is warmed or cooled by 3% of the global-mean SST anomaly in RCP8.5 compared to the pre-industrial control simulation for each year. The 3% anomaly applied to each region is inspired by the magnitude of AO-GCM error in simulating SST trends over the last few decades. For reference, 3% of the global-mean temperature anomaly for each year is plotted in Figure S5 of Supporting Information S1. While 3% is a small value, we concentrate this anomaly into a region of interest. For example, by 2085, a 3% anomaly of the global-mean SST change in the RCP8.5 simulation is about 0.06 K but becomes 1.1 K when that 0.06 K anomaly

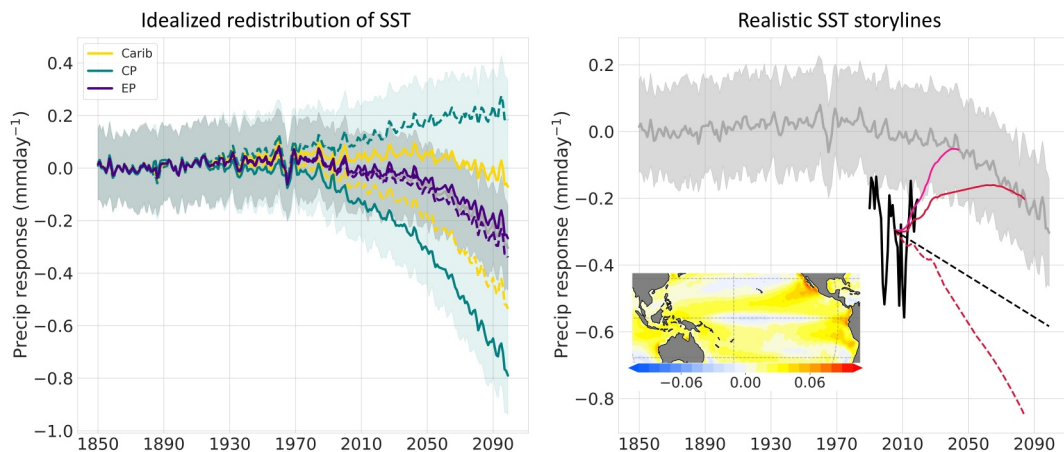


Figure 3. (left) Effect of idealized redistribution of sea surface temperature (SST) on SWUS precipitation. SWUS precipitation anomaly from the 1850–1870 average: MPI-GE historical and RCP8.5 projection ensemble-mean (gray); MPI-GE historical and RCP8.5 ensemble spread ($\pm 1\sigma$; gray shading); (right) Effect of adjusting SST trends starting from observations. SWUS precipitation anomaly from the 1850–1870 average: MPI-GE historical and RCP8.5 projection ensemble-mean (gray; as in a, note different range in vertical axis); MPI-GE historical and RCP8.5 ensemble spread ($\pm 1\sigma$; gray shading); HadISST convolved with the SWUS GF_p (black); precipitation response from transition SST scenarios starting from observed SST and ending with MPI-GE RCP8.5 SST over 10 years (dark pink), 50 years (red) and 50 years with the trend in the Central Pacific replaced by the 1991–2021 observed trend (dashed red); observed 1991–2021 SST trend convolved with the regional precipitation GF extended through 2100 (dashed black). The SST trend for the 50-year transition SST scenario (red) is plotted in the inset figure in units of K yr^{-1} .

is concentrated into a region of interest (e.g., the Central Pacific), which is comparable to model error in the tropical East Pacific (Figure 1 in Seager et al. (2019)) and the Southern Ocean (Figure 2 in Wills et al. (2022)). To maintain the same global-mean SST anomaly in the scenario as in the RCP8.5 simulation, the SST at other grid points around the globe, outside the region of interest, is slightly adjusted (an area-weighted cooling is applied to the rest of the world for a warming scenario, and vice-versa for a cooling storyline). Alessi and Rugensteiner (2023b) apply this method to net top-of-atmosphere radiative imbalance (see more details in Text S3 of Supporting Information S1).

Adjusting the SST trend in different regions by a modest amount significantly affects the SWUS precipitation trend (Figure 3a). As expected, changes in Central Pacific SST trends affect SWUS precipitation trends the most via changes in the midlatitude Rossby wave train, which can lengthen the subtropical Pacific jet, bringing more or less precipitation to the SWUS. The precipitation, 500 mb geopotential height, and specific humidity response to a warm anomaly patch simulation in the Central Pacific demonstrates increased precipitation and specific humidity as a result of a more prominent trough over the SWUS (bottom row in Figure S4 of Supporting Information S1). We find that SWUS precipitation decreases by 0.44 mm day^{-1} over the SWUS by 2085 compared to the standard coupled model projections due solely to a nearly 1.1 K decrease in Central Pacific SST. This is on the same order of magnitude as in the AO-GCM simulations from Delworth et al. (2015). Adjusting the SST trend in the Caribbean leads to an opposite and weaker SWUS precipitation response than warming or cooling in the Central Pacific. In empirical orthogonal function analysis of observations, there is some indication of the Caribbean having an opposite impact to the Central Pacific on SWUS precipitation during the spring season (Figure 3 in Hu et al. (2021)). The response of a Caribbean warm anomaly patch forcing is a decrease in SWUS precipitation linked to lower specific humidity because of a lack of northward moisture transport (Figure S4 in Supporting Information S1), possibly inhibiting the North American monsoon. Instead of moisture moving into the SWUS during the boreal summer, this moisture is instead focused over the region of warming, where more precipitation occurs. However, in one paleoclimate study, a decrease in SST in the Gulf of California resulted in less precipitation in the SWUS due to decreased northward surges of tropical moisture (Barron et al., 2012), which contradicts our GF and patch simulation result. We attribute this difference to a different North American monsoon structure: Barron et al. (2012) investigates monsoon proxies from 8,000 years ago, while we are using a climate model that simulates the North American monsoon in the present and future climate (Hernandez &

Chen, 2022). Finally, changing the East Pacific SST trend does little in impacting SWUS precipitation as expected from Figure 2a.

Critically, the SWUS could experience opposite trends in precipitation (wetting or drying) based on a small redistribution of SST. For example, if the Central Pacific (Caribbean) warms more than what AO-GCMs predict, indicative of a background mean-state El Niño, the SWUS would experience a wetting (drying) trend. On the other hand, if the Central Pacific (Caribbean) cools more than what AO-GCMs predict, the SWUS would experience a drying (wetting) trend. We applied these SST redistributions to the SST fields of all 100 MPI-GE ensembles members and took the ensemble-average after calculating the precipitation response to remove the impact of internal atmospheric variability. While atmospheric variability can be more important in affecting SWUS precipitation than SST forcing (compare the width of shading in Figure 3a to the magnitude of the mean response), we demonstrate here that in the ensemble-mean, the overall precipitation trend shifts based on the SST pattern trend, making it easier or more difficult for a precipitation deficit to develop in the SWUS.

Without any SST adjustment, the MPI-GE ensemble-mean predicts a slight drying over the 21st century (Figure 3a; gray line). This is due to a slow expansion of the Hadley Cell and a poleward shift of the subtropical dry zone (e.g., Grise & Davis, 2020; Lau & Kim, 2015). For other CMIP5 models, little precipitation change is projected in the model-mean for the SWUS, although there is considerable spread among the models (Rojas et al., 2019).

3.2. SST Storylines Starting From Observations

The SWUS precipitation response from the observed SST pattern (HadISST) convolved with the GF_p over the last few decades is noticeably lower than the MPI-GE (Figure 3b, black line). This demonstrates the GF_p 's ability to replicate the observed decrease in SWUS precipitation that led to drought conditions since the start of the 21st century.

Given that there is already a discrepancy between the observed and simulated SST trend pattern, we develop a more realistic SST pattern trend storyline that evolves from the currently observed SST pattern into the future. This storyline approach constrains future SWUS precipitation projections to be consistent with both the currently observed SST pattern and how we expect the SST pattern to evolve based on theory. The East Pacific is likely to switch from a cooling trend (1990–2020) to a warming trend at some point in the future as greenhouse gas forcing continues and aerosol forcing decreases (e.g., Andrews et al., 2022; Heede & Fedorov, 2021; Heede et al., 2020; Park et al., 2022), and in fact trends starting in the late 1990s are already positive. To reproduce this effect, we interpolate the observed SST at each grid point from the 2016–2021 average to the average SST pattern in the MPI-GE RCP8.5 for 2031–2036 and 2071–2076 (Figure 3b; Text S4 in Supporting Information S1). This interpolation includes a stronger warming of the subtropical East Pacific and Central Pacific than the equatorial West Pacific (Figure 3b inset), which is opposite of the trends observed since the 1970s. We choose two transition storylines, one 10 years in length (2021–2031) and one 50 years in length (2021–2071), since it is unknown how quickly or when the East Pacific may warm. These storylines assume that we trust the response of the models in the 2030s or 2070s. Below, we also relax this assumption. Both transition storylines result in increased precipitation for the SWUS over the next few decades. The 10-year transition storyline experiences a faster wetting than the 50-year transition storyline due to a faster warming in the Central and East Pacific. However, for both scenarios, after a period of wetting occurs due to the warming Central and East Pacific, the drying from the expanding Hadley Cell takes over as the transition storylines merge with the MPI-GE. For both storylines, while there is some warming in the Caribbean, the greater warming in the Tropical Pacific and higher sensitivity of SWUS precipitation to this region (Figure 2a) results in an overall wetting. Of note is the abrupt increase in SWUS precipitation for the transition storylines. We calculate the rate of change in SWUS precipitation for each ensemble member for all 20-year segments centered on 2025–2044 (in total there are twenty 20-year segments). The ensemble-mean rate of change in precipitation is $-0.00120 \text{ mm day}^{-1} 20 \text{ yr}^{-1}$ for RCP8.5 and $0.00125 \text{ mm day}^{-1} 20 \text{ yr}^{-1}$ for the 50-year transition storyline, indicating a greater (and positive) rate of change in SWUS precipitation for the storyline. If the observed SST trend pattern were to reverse in the Central and East Pacific from a cooling trend to a warming trend, as in the transition storylines, we may for several decades observe a wetting of the SWUS in spite of global warming. Note that this might happen independent of whether changes in the trends are due to decadal-scale internal variability or the forced response.

We develop two more storylines that assume SST projections from the RCP8.5 MPI-GE are either partly or fully incorrect. The first storyline is the same as the 50-year transition storyline in that the SST at each grid point is interpolated from observations to the RCP8.5 in 2071, however, the SST trend in the Central Pacific is replaced with the extrapolated 1991–2021 observed SST cooling trend through the end of the century (Figure 3b; dashed red line). In this storyline, we assume the AO-GCMs continue to incorrectly simulate the trend in the Central Pacific, and that the SST trend will continue to cool slightly (Seager et al., 2019). The difference between the dashed red line and the solid red line in Figure 3b is solely the influence of the Central Pacific cooling rather than warming. Despite warming across the rest of the globe, a cooling Central Pacific would result in continued drying for the SWUS, given its significant sensitivity to SST trends in that region (Section 3.1).

For the second storyline, we extrapolate the 30-year observed SST trend from 1991 to 2021 forward in time at each grid point (Figure 3b; black dashed line). We discard RCP8.5 SST pattern trend projections completely, or in other words, we do not trust the AO-GCM SST pattern trend at all. The extrapolated observed trend features a cooling Central and East Pacific, which results in a decreasing SWUS precipitation trend that remains below RCP8.5 projections through the end of the century. This storyline remains wetter than the combined 50-year transition and observed Central Pacific storyline due to the latter including warming in the Caribbean, which enhances the drying signal of that scenario. Overall global warming is significantly less in this storyline due to a more stabilizing global-mean radiative feedback (Alessi & Rogenstein, 2023b), which could lead to less drying in the SWUS from the Hadley Cell not expanding as much as in RCP8.5 projections. We conclude that in the near-future, the pattern of SST trends is highly relevant for the sign and magnitude of projections of SWUS precipitation.

4. Discussion and Conclusions

There is skill in predicting the precipitation trend in the SWUS based on the Equatorial Pacific SST trend pattern (Figure 1c; Dettinger et al., 1998; Schubert et al., 2016; Seager & Hoerling, 2014). However, AO-GCMs fail to replicate the observed SST trend pattern in recent decades (e.g., Wills et al., 2022). While AO-GCMs predicted a warming SST trend in the Central and East Pacific, the region instead experienced a cooling SST trend from 1970 to 2014 (e.g., Coats & Karnauskas, 2017; Seager et al., 2019), which potentially led to the observed megadrought in the SWUS due to a decrease in precipitation (Delworth et al., 2015; Seager & Hoerling, 2014). The cooling of the Central and East Pacific not simulated by AO-GCMs may have been caused by a forced response to greenhouse gas emissions (Coats & Karnauskas, 2017; Heede et al., 2020), a forced response to aerosols (Heede & Fedorov, 2021; Kuo et al., 2023), internal variability in the climate system (Olonscheck et al., 2020; Watanabe et al., 2021), missing or poorly simulated teleconnections in climate models (e.g., Y. Dong et al., 2022; Kang et al., 2023; Kim et al., 2022), or a combination of these factors. At least part of the megadrought was related to a lack of precipitation from the cooling Central and East Pacific, rather than due to a significant increase in evapotranspiration from global warming (Seager et al., 2015), which will likely cause droughts in the future as anthropogenic climate change worsens (e.g., Cook et al., 2014; Diffenbaugh et al., 2015). In this study, we confirmed the connection between the Equatorial Pacific SST trend pattern and SWUS precipitation trends with a Green's function approach, which allows us to establish a causal link between SST and precipitation. We developed SST pattern trend storylines to predict how SWUS precipitation could change over the next century:

A very modest redistribution of SST could lead to a wetting or drying of the SWUS using GF_P (Figure 3a). A warming of the Central Pacific results in a wetting of the SWUS due to a shift in deep tropical convection to the Central Pacific that excites the midlatitude Rossby wave such that the Pacific jet is extended into the SWUS, bringing moisture and precipitation (Figure S4 in Supporting Information S1). We also highlight a potentially strong teleconnection between the Caribbean and the SWUS, which may have been overlooked in the past due to weak warming and/or internal variability in studies based on regressions in observations. A warming of the Caribbean and Gulf of Mexico results in a drying of the SWUS due to a decrease in incoming moisture from the Caribbean (Figure S4 in Supporting Information S1), which could inhibit monsoon development (Ordoñez et al., 2019). The moisture instead remains in the Caribbean, fueling the increased convection due to the warmer SSTs.

The sign dependence of the SWUS precipitation trend on the SST trend pattern complicates prediction of future SWUS drought; since AO-GCMs are unable to replicate relevant aspects of the observed SST pattern trend, they may continue doing so in the future, confounding SWUS precipitation projections. This finding increases the total

uncertainty of SWUS precipitation in projections. Some models predict a wetting of the SWUS by the end of the century due to an extension of the Pacific jet stream, bringing in more precipitation to the SWUS (Deser et al., 2018; L. Dong & Leung, 2021; Grise & Davis, 2020). There also may exist a thermodynamic response which adds further uncertainty to subtropical land precipitation (He & Soden, 2017). Given that similar GF_P sensitivities exist in the GFDL model (Zhang et al., 2023) and the National Centers for Environmental Prediction model (Barsugli & Sardeshmukh, 2002), this result of the sign of SWUS precipitation trends being dependent on the Tropical Pacific SST is likely robust across AO-GCMs and a modest redistributions of SST trend patterns in the future will likely affect the sign of precipitation change in other AO-GCMs.

We note that internal atmospheric variability plays a large role in explaining interannual SWUS precipitation variance (e.g., Seager et al., 2015), so that even if the Central Pacific cools, the SWUS could experience a few wet years if atmospheric conditions are favorable. However, in long-term trends, all ensemble members still experience a drying in the SWUS if the Central Pacific cools (Figure 3a, solid teal line).

We also constrain projections of SWUS precipitation trends by developing storylines that start from the observed SST trend pattern (Figure 3b). If the Central and East Pacific continue cooling, a prolonged period of drought is more likely to continue in the SWUS. However, if the Central and East Pacific warm over the next few decades, as theory suggests (Heede et al., 2020), the SWUS would see a period of increased precipitation. This transition to a warming Central and East Pacific may have already begun (Andrews et al., 2022; Loeb et al., 2021; Rugenstein et al., 2023). Our approach does not consider changes in soil moisture and evaporative demand. The state of the hydroclimate overall could still experience drying with increased precipitation if there is a significant increase in evaporative demand, as suggested by models (Cook et al., 2014, 2015; Mankin et al., 2021; Schubert et al., 2016), though over the past 60 years evaporative demand may have had little impact (Sheffield et al., 2012).

Our work demonstrates that correctly modeled SST trend patterns are critical for SWUS precipitation projections. Improved and higher resolution modeling of ocean-atmosphere interaction may reduce mean-state biases and make the response to forcing more realistic in SST, allowing for more accurate simulation of Central and East Pacific SST trends. While AO-GCMs may fail to capture the future SST trend, and therefore the future SWUS precipitation trend, we here predict SWUS precipitation trends given likely storylines of future SST trend patterns. The possible wetting of the SWUS in the near-term should not deter efforts to limit water use and to prepare for significant drought in the SWUS, as there is ample evidence of increased drought under a drier overall hydroclimate due to anthropogenic climate change (Ault, 2020; Cook et al., 2014). However, a near-term wetting would bring relief to the drought stricken SWUS, which could prove crucial for adaptation and mitigation efforts in that region.

Data Availability Statement

Data for the MPI-GE historical and RCP8.5 SST, MPI-GE historical and RCP8.5 SWUS precipitation, GF_P response, and projections in Figure 3 can be found at Alessi and Rugenstein (2023a).

Acknowledgments

We thank Colin Evans and two anonymous reviewers for their comments on the manuscript. This work used resources of the Deutsches Klimarechenzentrum (DKRZ) granted by its Scientific Steering Committee (WLA) under project mh0066. MA and MR were supported through NSF EAR-2202916 and MR through NOAA NA23OAR4310596.

References

Alessi, M., & Rugenstein, M. (2023a). Potential near-term wetting of the Southwestern United States if the Eastern Pacific cooling trend reverses [Dataset]. Zenodo. <https://doi.org/10.5281/zenodo.10407741>

Alessi, M. J., & Rugenstein, M. A. A. (2023b). Surface temperature pattern scenarios suggest higher warming rates than current projections. *Geophysical Research Letters*, 50(23), e2023GL105795. <https://doi.org/10.1029/2023GL105795>

Andrews, T., Bodas-Salcedo, A., Gregory, J. M., Dong, Y., Armour, K. C., Paynter, D., et al. (2022). On the effect of historical SST patterns on radiative feedback. *Journal of Geophysical Research: Atmospheres*, 127(18), e2022JD036675. <https://doi.org/10.1029/2022JD036675>

Ault, T. R. (2020). On the essentials of drought in a changing climate. *Science*, 368(6488), 256–260. <https://doi.org/10.1126/science.aaz5492>

Barron, J. A., Metcalfe, S. E., & Addison, J. A. (2012). Response of the North American monsoon to regional changes in ocean surface temperature. *Paleoceanography*, 27(3), PA3206. <https://doi.org/10.1029/2011PA002235>

Barsugli, J. J., & Sardeshmukh, P. D. (2002). Global atmospheric sensitivity to tropical SST anomalies throughout the Indo-Pacific basin. *Journal of Climate*, 15(23), 3427–3442. [https://doi.org/10.1175/1520-0442\(2002\)015<3427:GASTTS>2.0.CO;2](https://doi.org/10.1175/1520-0442(2002)015<3427:GASTTS>2.0.CO;2)

Bloch-Johnson, J., Rugenstein, M. A. A., Alessi, M. J., Proistosescu, C., Zhao, M., Zhang, B., et al. (2024). The Green's function model intercomparison project (GFMIP) protocol. *Journal of Advances in Modeling Earth Systems*, 16(2), e2023MS003700. <https://doi.org/10.1029/2023MS003700>

Carrillo, C. M., Coats, S., Newman, M., Herrera, D. A., Li, X., Moore, R., et al. (2022). Megadrought: A series of unfortunate La Niña events? *Journal of Geophysical Research: Atmospheres*, 127(21), e2021JD036376. <https://doi.org/10.1029/2021JD036376>

Coats, S., & Karnauskas, K. B. (2017). Are simulated and observed twentieth century tropical Pacific sea surface temperature trends significant relative to internal variability? *Geophysical Research Letters*, 44(19), 9928–9937. <https://doi.org/10.1002/2017GL074622>

Cook, B. I., Ault, T. R., & Smerdon, J. E. (2015). Unprecedented 21st century drought risk in the American Southwest and Central Plains. *Science Advances*, 1(1), e1400082. <https://doi.org/10.1126/sciadv.1400082>

Cook, B. I., Mankin, J. S., Williams, A. P., Marvel, K. D., Smerdon, J. E., & Liu, H. (2021). Uncertainties, limits, and benefits of climate change mitigation for soil moisture drought in southwestern North America. *Earth's Future*, 9(9), e2021EF002014. <https://doi.org/10.1029/2021EF002014>

Cook, B. I., Seager, R., & Smerdon, J. E. (2014). The worst North American drought year of the last millennium: 1934. *Geophysical Research Letters*, 41(20), 7298–7305. <https://doi.org/10.1002/2014GL061661>

Cook, B. I., Williams, A. P., Mankin, J. S., Seager, R., Smerdon, J. E., & Singh, D. (2018). Revisiting the leading drivers of pacific coastal drought variability in the contiguous United States. *Journal of Climate*, 31(1), 25–43. <https://doi.org/10.1175/JCLI-D-17-0172.1>

Delworth, T. L., Zeng, F., Rosati, A., Vecchi, G. A., & Wittenberg, A. T. (2015). A link between the hiatus in global warming and North American drought. *Journal of Climate*, 28(9), 3834–3845. <https://doi.org/10.1175/JCLI-D-14-00616.1>

Deser, C., Simpson, I. R., Phillips, A. S., & McKinnon, K. A. (2018). How well do we know ENSO's climate impacts over North America, and how do we evaluate models accordingly? *Journal of Climate*, 31(13), 4991–5014. <https://doi.org/10.1175/JCLI-D-17-0783.1>

Dettinger, M. D., Cayan, D. R., Diaz, H. F., & Meko, D. M. (1998). North–South precipitation patterns in western North America on interannual-to-decadal timescales. *Journal of Climate*, 11(12), 3095–3111. [https://doi.org/10.1175/1520-0442\(1998\)011<3095:NPPIW>2.0.CO;2](https://doi.org/10.1175/1520-0442(1998)011<3095:NPPIW>2.0.CO;2)

Diffenbaugh, N. S., Swain, D. L., & Touma, D. (2015). Anthropogenic warming has increased drought risk in California. *Proceedings of the National Academy of Sciences*, 112(13), 3931–3936. <https://doi.org/10.1073/pnas.1422385112>

Dong, L., & Leung, L. R. (2021). Winter precipitation changes in California under global warming: Contributions of CO₂, uniform SST warming, and SST change patterns. *Geophysical Research Letters*, 48(5), e2020GL091736. <https://doi.org/10.1029/2020GL091736>

Dong, Y., Armour, K. C., Battisti, D. S., & Blanchard-Wrigglesworth, E. (2022). Two-way teleconnections between the Southern Ocean and the tropical Pacific via a dynamic feedback. *Journal of Climate*, 35(19), 6267–6282. <https://doi.org/10.1175/JCLI-D-22-0080.1>

Dong, Y., Proistosescu, C., Armour, K. C., & Battisti, D. S. (2019). Attributing historical and future evolution of radiative feedbacks to regional warming patterns using a Green's function approach: The preeminence of the western Pacific. *Journal of Climate*, 32(17), 5471–5491. <https://doi.org/10.1175/JCLI-D-18-0843.1>

Evans, C. P., Coats, S., Carrillo, C. M., Li, X., Alessi, M. J., Herrera, D. A., et al. (2022). Intrinsic century-scale variability in tropical Pacific sea surface temperatures and their influence on western US hydroclimate. *Geophysical Research Letters*, 49(23), e2022GL099770. <https://doi.org/10.1029/2022GL099770>

Grise, K. M., & Davis, S. M. (2020). Hadley cell expansion in CMIP6 models. *Atmospheric Chemistry and Physics*, 20(9), 5249–5268. <https://doi.org/10.5194/acp-20-5249-2020>

He, J., & Soden, B. J. (2017). A re-examination of the projected subtropical precipitation decline. *Nature Climate Change*, 7(1), 53–57. <https://doi.org/10.1038/nclimate3157>

Heede, U. K., & Fedorov, A. V. (2021). Eastern equatorial Pacific warming delayed by aerosols and thermostat response to CO₂ increase. *Nature Climate Change*, 11(8), 696–703. <https://doi.org/10.1038/s41558-021-01101-x>

Heede, U. K., Fedorov, A. V., & Burlis, N. J. (2020). Time scales and mechanisms for the tropical Pacific response to global warming: A tug of war between the ocean thermostat and weaker walker. *Journal of Climate*, 33(14), 6101–6118. <https://doi.org/10.1175/JCLI-D-19-0690.1>

Hernandez, M., & Chen, L. (2022). Future land precipitation changes over the North American monsoon region using CMIP5 and CMIP6 simulations. *Journal of Geophysical Research: Atmospheres*, 127(9), e2021JD035911. <https://doi.org/10.1029/2021JD035911>

Hoerling, M. P., & Kumar, A. (2002). Atmospheric response patterns associated with tropical forcing. *Journal of Climate*, 15(16), 2184–2203. [https://doi.org/10.1175/1520-0442\(2002\)015<2184:ARPAWT>2.0.CO;2](https://doi.org/10.1175/1520-0442(2002)015<2184:ARPAWT>2.0.CO;2)

Hoerling, M. P., Kumar, A., & Zhong, M. (1997). El Niño, La Niña, and the nonlinearity of their teleconnections. *Journal of Climate*, 10(8), 1769–1786. [https://doi.org/10.1175/1520-0442\(1997\)010<1769:ENOLNA>2.0.CO;2](https://doi.org/10.1175/1520-0442(1997)010<1769:ENOLNA>2.0.CO;2)

Horel, J. D., & Wallace, J. M. (1981). Planetary-scale atmospheric phenomena associated with the Southern Oscillation. *Monthly Weather Review*, 109(4), 813–829. [https://doi.org/10.1175/1520-0493\(1981\)109<0813:PSAPAW>2.0.CO;2](https://doi.org/10.1175/1520-0493(1981)109<0813:PSAPAW>2.0.CO;2)

Hu, F., Zhang, L., Liu, Q., & Chi, D. (2021). Environmental factors controlling the precipitation in California. *Atmosphere*, 12(8), 997. <https://doi.org/10.3390/atmos12080997>

Kang, S. M., Yu, Y., Deser, C., Zhang, X., Kang, I.-S., Lee, S.-S., et al. (2023). Global impacts of recent Southern Ocean cooling. *Proceedings of the National Academy of Sciences*, 120(30), e2300881120. <https://doi.org/10.1073/pnas.2300881120>

Kim, H., Kang, S. M., Kay, J. E., & Xie, S.-P. (2022). Subtropical clouds key to Southern Ocean teleconnections to the tropical Pacific. *Proceedings of the National Academy of Sciences*, 119(34), e2200514119. <https://doi.org/10.1073/pnas.2200514119>

Kuo, Y.-N., Kim, H., & Lehner, F. (2023). Anthropogenic Aerosols contribute to the recent decline in precipitation over the U.S. Southwest. *Geophysical Research Letters*, 50(23), e2023GL105389. <https://doi.org/10.1029/2023GL105389>

Lau, W. K. M., & Kim, K.-M. (2015). Robust Hadley Circulation changes and increasing global dryness due to CO₂ warming from CMIP5 model projections. *Proceedings of the National Academy of Sciences*, 112(12), 3630–3635. <https://doi.org/10.1073/pnas.1418682112>

Lehner, F., Deser, C., Simpson, I. R., & Terray, L. (2018). Attributing the U.S. Southwest's recent shift into drier conditions. *Geophysical Research Letters*, 45(12), 6251–6261. <https://doi.org/10.1029/2018GL078312>

Loeb, N. G., Johnson, G. C., Thorsen, T. J., Lyman, J. M., Rose, F. G., & Kato, S. (2021). Satellite and ocean data reveal marked increase in Earth's heating rate. *Geophysical Research Letters*, 48(13), e2021GL093047. <https://doi.org/10.1029/2021GL093047>

Mankin, J. S., Simpson, I., Hoell, A., Fu, R., Lisonbee, J., Sheffield, A., & Barrie, D. (2021). *NOAA drought task force report on the 2020–2021 Southwestern U.S. drought*. NOAA Drought Task Force, MAPP, and NIDIS.

McCabe, G. J., Palecki, M. A., & Betancourt, J. L. (2004). Pacific and Atlantic Ocean influences on multidecadal drought frequency in the United States. *Proceedings of the National Academy of Sciences*, 101(12), 4136–4141. <https://doi.org/10.1073/pnas.0306738101>

Olonscheck, D., Rogenstein, M., & Marotzke, J. (2020). Broad consistency between observed and simulated trends in sea surface temperature patterns. *Geophysical Research Letters*, 47(10), e2019GL086773. <https://doi.org/10.1029/2019GL086773>

Ordoñez, P., Nieto, R., Gimeno, L., Ribera, P., Gallego, D., Ochoa-Moya, C. A., & Quintanar, A. I. (2019). Climatological moisture sources for the western North American monsoon through a Lagrangian approach: Their influence on precipitation intensity. *Earth System Dynamics*, 10(1), 59–72. <https://doi.org/10.5194/esd-10-59-2019>

Park, C., Kang, S. M., Stuecker, M. F., & Jin, F.-F. (2022). Distinct surface warming response over the western and eastern equatorial Pacific to radiative forcing. *Geophysical Research Letters*, 49(2), e2021GL095829. <https://doi.org/10.1029/2021GL095829>

Piechota, T. C., & Dracup, J. A. (1996). Drought and regional hydrologic variation in the United States: Associations with the El Niño–Southern Oscillation. *Water Resources Research*, 32(5), 1359–1373. <https://doi.org/10.1029/96WR00353>

Redmond, K. T., & Koch, R. W. (1991). Surface climate and streamflow variability in the western United States and their relationship to large-scale circulation indices. *Water Resources Research*, 27(9), 2381–2399. <https://doi.org/10.1029/91WR00690>

Rojas, M., Lambert, F., Ramirez-Villegas, J., & Challinor, A. J. (2019). Emergence of robust precipitation changes across crop production areas in the 21st century. *Proceedings of the National Academy of Sciences*, 116(14), 6673–6678. <https://doi.org/10.1073/pnas.1811463116>

Ropelewski, C. F., & Halpert, M. S. (1986). North American precipitation and temperature patterns associated with the El Niño/Southern Oscillation (ENSO). *Monthly Weather Review*, 114(12), 2352–2362. [https://doi.org/10.1175/1520-0493\(1986\)114<2352:NAPATP>2.0.CO;2](https://doi.org/10.1175/1520-0493(1986)114<2352:NAPATP>2.0.CO;2)

Rugenstein, M., Dhame, S., Olonscheck, D., Wills, R. J., Watanabe, M., & Seager, R. (2023). Connecting the SST pattern problem and the hot model problem. *Geophysical Research Letters*, 50(22), e2023GL105488. <https://doi.org/10.1029/2023GL105488>

Sardeshmukh, P. D., & Hoskins, B. J. (1988). The generation of global rotational flow by steady idealized tropical divergence. *Journal of the Atmospheric Sciences*, 45(7), 1228–1251. [https://doi.org/10.1175/1520-0469\(1988\)045<1228:TGOGRF>2.0.CO;2](https://doi.org/10.1175/1520-0469(1988)045<1228:TGOGRF>2.0.CO;2)

Schubert, S. D., Stewart, R. E., Wang, H., Barlow, M., Berbery, E. H., Cai, W., et al. (2016). Global meteorological drought: A synthesis of current understanding with a focus on SST drivers of precipitation deficits. *Journal of Climate*, 29(11), 3989–4019. <https://doi.org/10.1175/JCLI-D-15-0452.1>

Seager, R., Cane, M., Henderson, N., Lee, D.-E., Abernathey, R., & Zhang, H. (2019). Strengthening tropical Pacific zonal sea surface temperature gradient consistent with rising greenhouse gases. *Nature Climate Change*, 9(7), 517–522. <https://doi.org/10.1038/s41558-019-0505-x>

Seager, R., & Hoerling, M. (2014). Atmosphere and ocean origins of North American droughts. *Journal of Climate*, 27(12), 4581–4606. <https://doi.org/10.1175/JCLI-D-13-00329.1>

Seager, R., Hoerling, M., Schubert, S., Wang, H., Lyon, B., Kumar, A., et al. (2015). Causes of the 2011–14 California drought. *Journal of Climate*, 28(18), 6997–7024. <https://doi.org/10.1175/JCLI-D-14-00860.1>

Seager, R., Naik, N., & Vecchi, G. A. (2010). Thermodynamic and dynamic mechanisms for large-scale changes in the hydrological cycle in response to global warming. *Journal of Climate*, 23(17), 4651–4668. <https://doi.org/10.1175/2010JCLI3655.1>

Sheffield, J., Wood, E. F., & Roderick, M. L. (2012). Little change in global drought over the past 60 years. *Nature*, 491(7424), 435–438. <https://doi.org/10.1038/nature11575>

Watanabe, M., Dufresne, J.-L., Kosaka, Y., Mauritsen, T., & Tatebe, H. (2021). Enhanced warming constrained by past trends in equatorial Pacific sea surface temperature gradient. *Nature Climate Change*, 11(1), 33–37. <https://doi.org/10.1038/s41558-020-00933-3>

Williams, A. I. L., Jeevanjee, N., & Bloch-Johnson, J. (2023). Circus tents, convective thresholds, and the non-linear climate response to tropical SSTs. *Geophysical Research Letters*, 50(6), e2022GL101499. <https://doi.org/10.1029/2022GL101499>

Williams, A. P., Cook, B. I., & Smerdon, J. E. (2022). Rapid intensification of the emerging southwestern North American megadrought in 2020–2021. *Nature Climate Change*, 12(3), 232–234. <https://doi.org/10.1038/s41558-022-01290-z>

Wills, R. C. J., Dong, Y., Proistosecu, C., Armour, K. C., & Battisti, D. S. (2022). Systematic climate model biases in the large-scale patterns of recent sea-surface temperature and sea-level pressure change. *Geophysical Research Letters*, 49(17), e2022GL100011. <https://doi.org/10.1029/2022GL100011>

Zhang, B., Zhao, M., & Tan, Z. (2023). Using a Green's function approach to diagnose the pattern effect in GFDL AM4 and CM4. *Journal of Climate*, 36(4), 1105–1124. <https://doi.org/10.1175/JCLI-D-22-0024.1>

Zhou, C., Zelinka, M. D., & Klein, S. A. (2017). Analyzing the dependence of global cloud feedback on the spatial pattern of sea surface temperature change with a Green's function approach. *Journal of Advances in Modeling Earth Systems*, 9(5), 2174–2189. <https://doi.org/10.1002/2017MS001096>

References From the Supporting Information

Fueglistaler, S., & Silvers, L. G. (2021). The peculiar trajectory of global warming. *Journal of Geophysical Research: Atmospheres*, 126(4), e2020JD033629. <https://doi.org/10.1029/2020JD033629>

Rayner, N. A., Parker, D. E., Horton, E. B., Folland, C. K., Alexander, L. V., Rowell, D. P., et al. (2003). Global analyses of sea surface temperature, sea ice, and night marine air temperature since the late nineteenth century. *Journal of Geophysical Research*, 108(D14), 4407. <https://doi.org/10.1029/2002JD002670>

Stevens, B., Giorgetta, M., Esch, M., Mauritsen, T., Crueger, T., Rast, S., et al. (2013). Atmospheric component of the MPI-M Earth System Model: ECHAM6. *Journal of Advances in Modeling Earth Systems*, 5(2), 146–172. <https://doi.org/10.1002/jame.20015>